International Journal of Sustainable and Green Energy
2015; 4(6): 219-226
Published online November 23, 2015 (http://www.sciencepublishinggroup.com/j/ijsge)
doi: 10.11648/j.ijrse.20150406.13

Dye-Sensitized Solar Cell Using Copper and Nitrogen Co-doped Titania as Photoanode

Purnima Dashora, Chetna Ameta, Rakshit Ameta, Suresh C. Ameta*

Department of Chemistry, PAHER University, Udaipur, (Raj.) India

Email address:
purnimadashora@gmail.com (P. Dashora), ameta_sc@yahoo.com (S. C. Ameta)

To cite this article:
Purnima Dashora, Chetna Ameta, Rakshit Ameta, Suresh C. Ameta. Dye-Sensitized Solar Cell Using Copper and Nitrogen Co-doped Titania as Photoanode. *International Journal of Sustainable and Green Energy.* Vol. 4, No. 6, 2015, pp. 219-226. doi: 10.11648/j.ijrse.20150406.13

Abstract: Energy crisis is a burning problem in the present scenario, as natural energy resources will be exhausted very soon, due to their rapid utilization. Solar cells have attracted the attention of researchers, as using these devices sunlight can be converted into electricity, which is freely available to us. DSSCs is one of the important and new type of solar cell, which deliver higher photoelectric conversion efficiency and low production cost by combining wide-band gap semiconductor electrode, dye as sensitizer, a counter electrode and redox electrolyte like iodide and triiodide ions between them. In the present work, a comparison is made for the efficiency of pure TiO_2 and Cu/N co-doped TiO_2 fabricated DSSCs. Pure TiO_2 and Cu/N co-doped TiO_2 were prepared through sol-gel process. These electrodes were also characterized by X-ray diffraction (XRD), scanning electron microscopy (SEM), fourier transform infrared (FTIR), transmission electron microscopy (TEM) and diffuse reflectance spectra (DRS) techniques to know about their morphology, band gap, particle size etc. The cell was prepared by coating of Cu/N–TiO_2 film on the conductive side of FTO glasses using Rhodamine B dye as sensitizer. Liquid electrolyte I^-/I_3^- redox couple and carbon (graphite) as counter electrode and light intensity 60 $mWcm^{-2}$ were used. The observations revealed that Cu/N doped electrode showed maximum conversion efficiency with an open circuit voltage (V_{oc}) = 395.0 mV, short circuit current (i_{sc}) = 0.0339 mA, V_{pp} = 66.2 mV and i_{pp} = 0.0209 mA with fill factor = 0.10 and the power conversion efficiency (η) = 0.0023%, which is higher than that of pure TiO_2. The results showed that the doping of TiO_2 by copper and nitrogen improved the efficiency of this solar cell 38 times more in compare to pure TiO_2.

Keywords: Titania, Photoanode, Dye-Sensitized Solar Cell, Co-doped, Photovoltaic Performance

1. Introduction

In coming few decades, renewable energy especially solar energy, has attracted much attention because it offers a clean, environment-friendly, abundant, and infinite energy resource to us. A solar cell directly converts solar energy into electrical power using a semiconductor. Among all the organic cells, dye sensitized solar cells (DSSCs) provide more effective method because of their high conversion efficiency, low cost, easy manufacturing process, and non-toxicity. DSSC has five main components ─ transparent conducting glass, semiconductor materials, dyes as a sensitizer, redox-couple electrolyte and counter electrode. The principle of DSSCs was firstly reported by Gratzel and O' Regan using TiO_2 films. The electrical conversion efficiency in simulated solar light is about 7.1-7.9% and 12% in diffuse daylight [1]. Chiba et al obtained 11.1% conversion efficiency using titania electrodes with different haze. It indicates that conversion efficiency of the cell increases with increase in the haze of TiO_2 electrodes [2]. Different approaches have been attempted to achieve higher power conversion efficiency such as co-sensitization, core-shell microspheres, composite nanoparticles [3, 4, 5].

Various doping process have been used to enhance the activity of the semiconducting materials. A strong red shift in the visible light region has been observed by doped semiconductors as compared to undoped semiconductor [6]. Gu et al. reported that there is improvement in open-circuit voltage due to an upward shift of the Fermi level, but the oxygen defects generated retard the negative shift of the Fermi level [7]. Modification of TiO_2 electrode by doping with metal and non-metal such as chromium, nickel, nitrogen, fluorine, and iodine doped $TiO_2$was made by Xie et al. [8], Chou et al. [9] and Niu et al. [10]. A scattering layer and a nano-crystalline TiO_2 electrode layer was fabricated using of Er^{3+} and Yb^{3+} co-doped TiO_2, which showed better light scattering as well as lower transmittance property. The light scattering layer increased the efficiency of the DSSC to

by 15.6% [11]. Sn/F dual doping with TiO_2 was proposed by Duan et al. and the power conversion efficiency was about 8.89% which is higher than the undoped TiO_2 [12].

In the present work, Cu/N-TiO_2 was synthesized by sol-gel method and the electric output of the cell was examined using different parameters such as dye concentration, electrolyte concentration, light intensity, and surface area of semiconductor.

2. Experimental

2.1. Preparation of Pure and Doped TiO_2

Both pure and co-doped Cu/N─TiO_2 were synthesized by using sol-gel method. It is schematically presented in Fig 1.

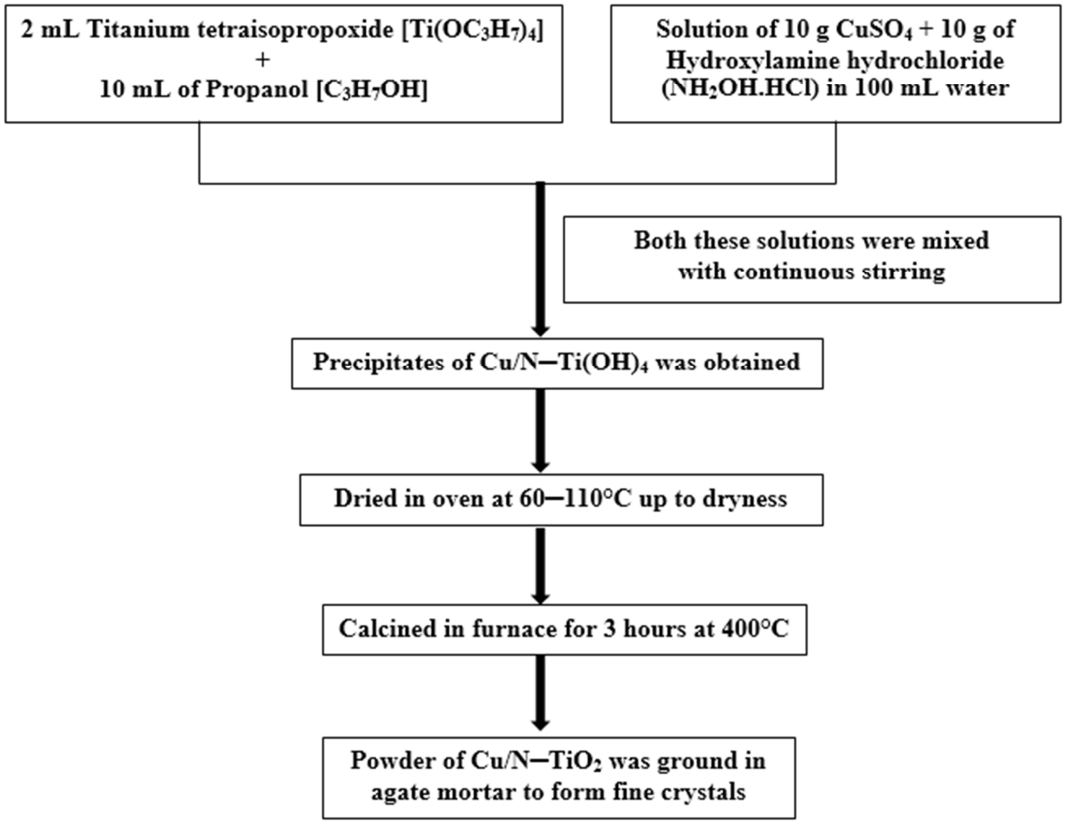

Fig. 1. *Sol-gel method for the preparation of doped TiO_2.*

The same procedure was followed to prepare for undoped TiO_2 with the only difference that in this case, no dopant was added.

2.2. Fabrication of Cell

The working electrode was prepared with Cu/N─TiO_2 paste in acetic acid with few drops of dishwashing liquid as a surfactant. This paste was coated on the FTO glass (2.2 mm thickness, 7-9 ohm cm^{-2}, L 25 mm x W 25 mm, Shilpa Enterprises, Nagpur, India) by doctor blade method and left for a few minutes to let it dry. Then the glass was heated on a hot plate at 100°C for 45 min. Rhodamine B (1.0×10^{-3} M) dye solution was prepared in ethanol and used as a sensitizer for the working electrode. The working electrode was dipped in dye solution for 15 min. and then rinsed with ethanol to remove extra dye. A counter electrode, coated with carbon (graphite) was clipped onto the top of the working electrode. 0.47 M iodine and 0.51 M potassium iodide was dissolved in 10 mL of ethylene glycol. This I^-/I_3^- redox couple was used as liquid electrolyte.

3. Characterization of Semiconductors

3.1. FTIR Spectra of Doped Cu/N─TiO_2

The Fourier transform infrared (FTIR) spectrum of the synthesized samples were recorded in potassium bromide (KBr) pellets on a Perkin Elmer Spectrum RX1 spectrometer in the range from 4000 cm^{-1} to 400 cm^{-1} at a scanning rate of cm^{-1}/min.

The FTIR spectrum of Cu/N–TiO_2 in given Fig. 2. The broad band at 3365-3318 cm^{-1} was due to O–H stretching. The peak between at 1630-1622 cm^{-1} was attributed to O–H bending vibration of adsorbed water molecule and hydroxyl groups on the surface of TiO_2 [13]. The peaks at 494-433 cm^{-1} and 731-702 $cm^{-1}$are due to bending and stretching mode of Ti–O–Ti [14]. In the low frequency region, the bands around 585-525 cm^{-1} were attributed to the Cu–O and Cu–Ti stretching vibration and 604-625 $cm^{-1}$to Cu–N–O bending [15, 16]. A typical absorption band occurred

around 1092-1016 cm^{-1} belonging to Ti–N stretch vibrations and new peaks in the range of 1153-1115 cm^{-1} and 1118-1198 cm^{-1} appeared due to N–TiO_2 [17, 18]. The bands of O–Ti–O and Ti–O appeared at 625-616 cm^{-1} and 660-626 cm^{-1} [19].

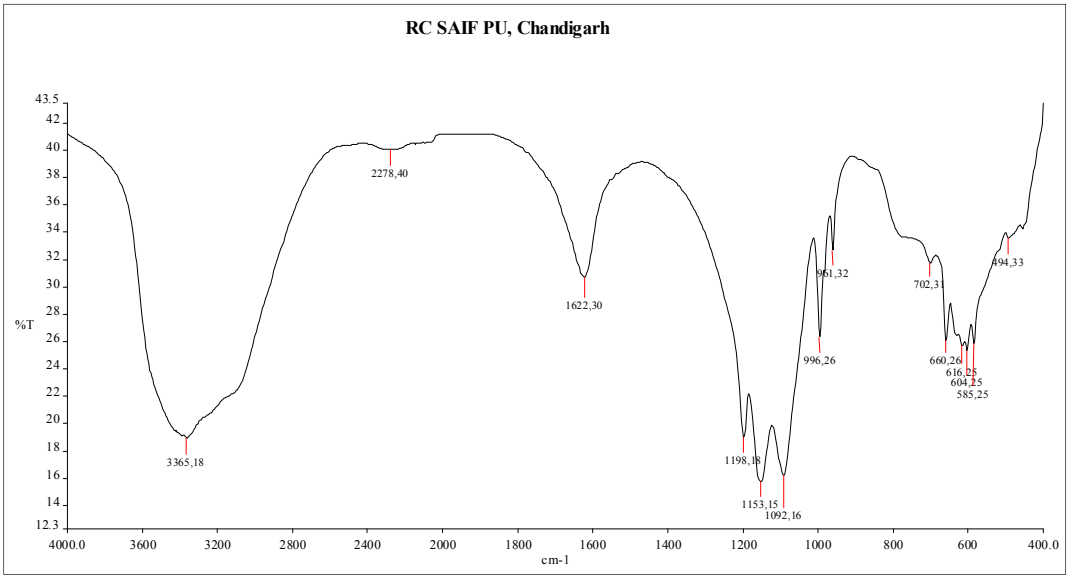

Fig. 2. *FTIR spectrum of doped Cu/N─TiO_2.*

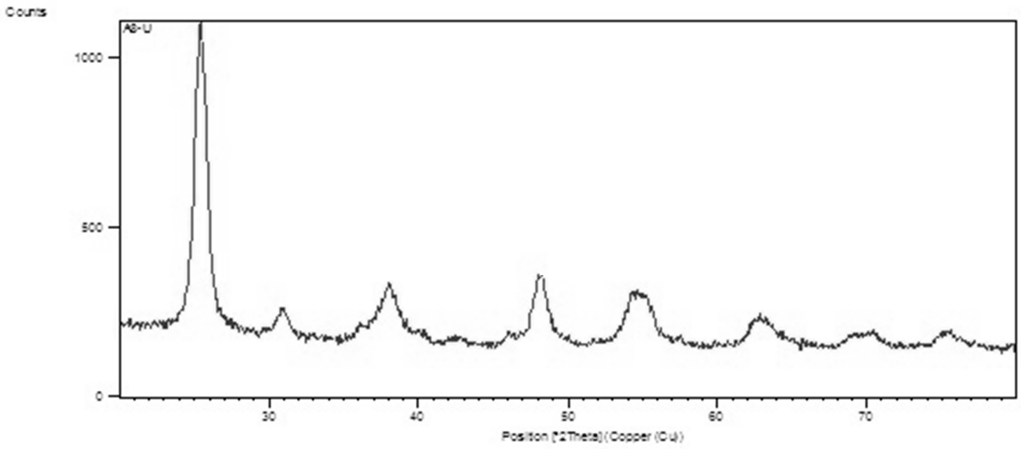

Fig. 3. *XRD of undoped TiO_2.*

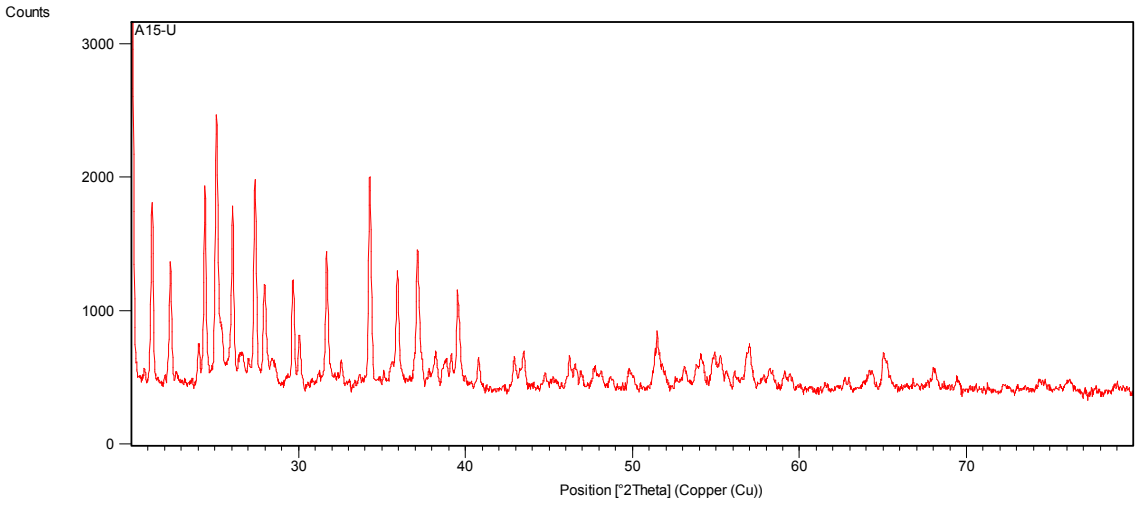

Fig. 4. *XRD of Cu/N–TiO_2.*

3.2. X-ray Diffraction

The X-ray diffraction of undoped TiO_2 and Cu/N–TiO_2 samples are given in Fig. 3 and 4. The XRD patterns were recorded on Panlytical X' pert Pro model X-ray diffraction using Cu Kα radiation as the X-ray source. The diffractograms were recorded in the 2θ range of 20-80°. The average crystalline size (D) of the undoped and Cu/N–TiO_2 material can be calculated from the Debye–Scherrer formula:

$$D = \frac{K\lambda}{\beta \cos\theta} \quad (1)$$

Where D is the crystalline size (nm), λ is the wavelength of X-ray source (λ = 0.1540 nm for CuKα), β is the full width at half maximum intensity (FWHM–in radian), and θ is the Bragg diffraction angle (°). It is also confirmed by the spectra that both; undoped and doped TiO_2 are crystalline in nature. The average crystalline size of the pure TiO_2 was 10.15 nm and Cu/N–TiO_2 was 86.62 nm. It was observed that after doping, the particle size increases.

3.3. Scanning Electron Microscopy (SEM)

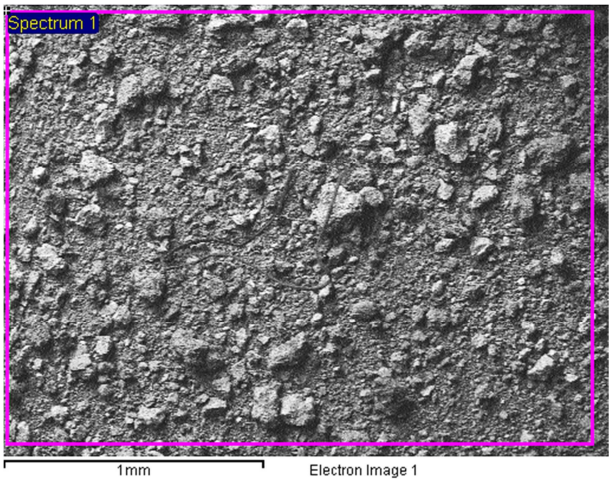

Fig. 5. *SEM of Cu/N–TiO_2*

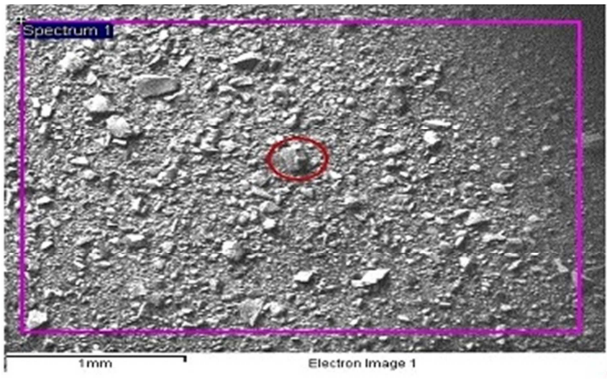

Fig. 6. *SEM of Undoped TiO_2.*

Fig. 5 and 6 show SEM images of Cu–N doped TiO_2 and undoped TiO_2. SEM has been used to observe the morphological changes caused by loading of metal and non-metal on the surface of titania. It was observed that combination of the dopants Cu and N on TiO_2 increases particle size.

3.4. Transmission Electron Microscopy (TEM)

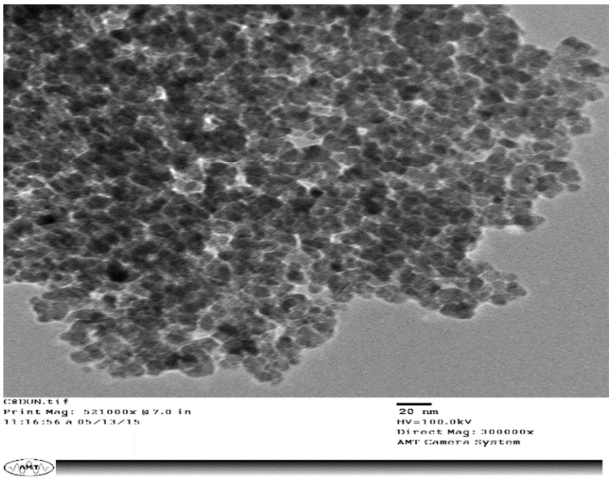

Fig. 7. *TEM of undoped TiO_2.*

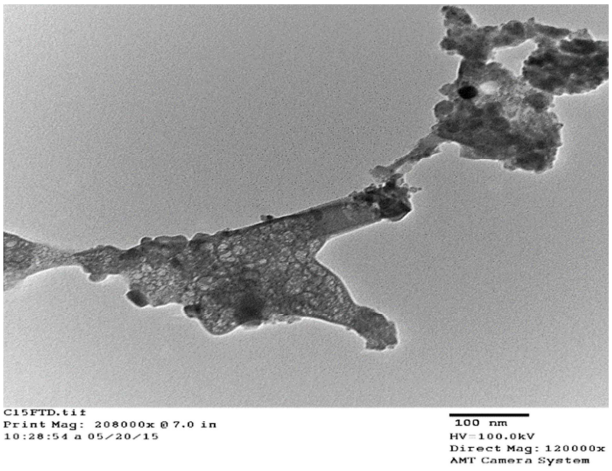

Fig. 8. *TEM of Cu/N–TiO_2.*

Fig. 7 and 8 show TEM images of pure and co-doped TiO_2. Doping of TiO_2 is clearly observed as evident from some lumps in co-doped TiO_2, which is absent in undoped TiO_2

3.5. Diffuse Reflectance Spectrum (DRS)

The diffuse reflectance spectrum was scanned between 200-800 nm using UV Vis-3000 + spectrophotometer. It shows an intense absorption in the visible region at 739 nm. The band gap of co-doped TiO_2 was calculated to be 1.67 eV, which is much less than undoped TiO_2 (3.2 eV).

4. Performance of Dssc

4.1. Variation of Potential with Time

The effect of potential with time on the electrical output of

the cell was observed and results are reported in Table 1. The cell was placed in dark and the potential was measured after it becomes stable. A change in potential with the time was observed, when the cell was exposed in light (60 $mWcm^{-2}$). The potential was measured with digital multimeter (Mastech-M830bZ). The cell was charged for 70 min. and then light was cut off. It was observed that the potential was increased with increasing time.

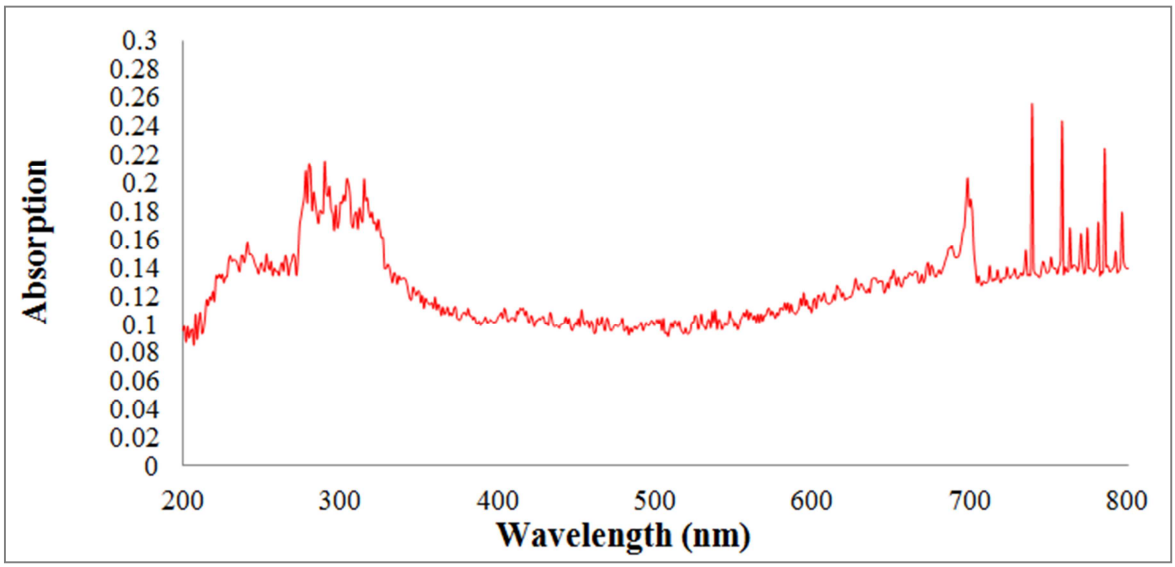

Fig. 9. *DRS of Cu/N–TiO_2.*

Table 1. *Variation of potential with time.*

Time (min.)	Potential (mV)	Time (min.)	Potential (mV)
0.0	-395.0	75	-18.7
5	-253.2	80	-17.8
10	-230.7	85	-17.5
15	-203.6	90	-17.2
20	-187.8	95	-16.9
25	-118.5	100	-16.5
30	-91.9	105	-15.9
35	-66.0	110	-14.8
40	-48.9	115	-14.1
45	-39.6	120	-13.7
50	-34.0	125	-13.7
55	-29.1	130	-12.2
60	-22.0	135	-12.2
65	-16.1	140	-12.2
70 (Light off)	-16.1		

[Rhodamine B] = 1.0 x 10^{-3}M; Electrolyte [I_2] = 0.47 M, [KI] = 0.51 M; Exposed surface area = 1.0 x 1.0 cm^2; Light intensity = 60 $mWcm^{-2}$

4.2. Variation of Current with Time

The effect of current with time on the electrical output of the cell was observed and results are summarized in Table 2. The current was also measured by digital multimeter (Mastech-M830bZ). The current of cell increases rapidly and in few minutes, it reaches its maximum, which is represented as i_{max}. When irradiation time was increased further, current starts decreasing steadily and reaches almost a stable (constant value). This value is represented as i_{eq}, when the source of light was removed, the current starts decreasing further.

Table 2. *Variation of current with time.*

Time (min.)	Current (µA)	Time (min.)	Current (µA)
0.0	12.8	75	14.3
5	20.6	80	13.7
10	41.2	85	12.9
15	76.6 ($i_{max.}$)	90	12.3
20	56.6	95	12.1
25	51.7	100	10.4
30	46.5	105	9.2
35	40.1	110	8.7
40	34.9	115	8.5
45	29.0	120	8.3
50	25.8	125	8.1
55	21.5	130	8.0
60	17.6	135	8.0
65	15.9	140	8.0
70 (Light off)	15.0 ($i_{eq.}$)		

[Rhodamine B] = 1.0 x 10^{-3} M; Electrolyte [I_2] = 0.47 M, [KI] = 0.51 M; Exposed surface area = 1.0 x 1.0 cm^2; Light intensity = 60 $mWcm^{-2}$

4.3. Effect of Dye Concentration

The potential and current of the cell was observed using different concentrations (1.6 x 10^{-3} M – 0.3 x 10^{-3} M) of dye. The results are given in Table 3. It was observed that as the concentration of dye was increased, the number of sensitizer molecules also increases but above 1.0 x 10^{-3}M, both the current as well as potential were found to decrease.

Table 3. *Effect of dye concentration.*

Dye (10^3M)	Potential (mA)	Current (µA)
0.3	292.4	15.9
0.6	319.8	27.8
1.0	395.0	33.9
1.3	379.7	31.5
1.6	318.2	23.6

Electrolyte [I_2] = 0.47 M, [KI] = 0.51 M; Exposed surface area = 1.0 x1.0 cm^2; Light intensity = 60 $mWcm^{-2}$

4.4. Effect of Electrolyte Concentration

The effect of the concentration of liquid electrolyte (I_2 and KI) on the performance of the DSSC was observed, and the results are presented in Table 4. The concentration of one component was kept constant and other was varied to know the effect of components of redox couple, I_2 and KI. As the concentration of iodine was increased; both, the potential and current were increased but above 0.47 M, the current and potential were found to decrease. When the potassium iodide concentration was increased, both the current and potential were increased. The optimum conditions for I_2 and KI were obtained as 0.47 M and 0.51 M.

Table 4. *Effect of I_2 concentration.*

I_2 (M)	Potential (mA)	Current (µA)
0.39	220.1	11.7
0.43	312.0	23.3
0.47	395.0	33.9
0.51	219.6	28.1
0.55	153.7	13.0

Exposed surface area = 1.0 x1.0 cm^2; Light intensity = 60 $mWcm^{-2}$; [Rhodamine B] = 1.0 x 10^{-3}M

Table 5. *Effect of KI concentration.*

KI (M)	Potential (mA)	Current (µA)
0.44	129.9	9.7
0.46	197.5	15.9
0.48	216.4	22.9
0.50	273.9	26.3
0.51	395.0	33.9

Exposed surface area = 1.0 x1.0 cm^2; Light intensity = 60 $mWcm^{-2}$; [Rhodamine B] = 1.0 × 10^{-3}M

4.5. Effect of Surface Area of Electrode

Table 6. *Effect of exposed surface area.*

Area (cm^2)	Potential (mA)	Current (µA)
0.6 x 0.6	203.1	24.2
1.0 x 1.0	395.0	33.9
1.3 x 1.3	257.0	19.4
1.6 x 1.6	121.2	14.8

[Rhodamine B] = 1.0 x 10^{-3} M; Light intensity = 60 $mWcm^{-2}$; Electrolyte [I_2] = 0.47 M, [KI] = 0.51 M.

The performance of the cell may also be affected by the area of the semiconductor. Its effect was observed by changing the surface area of the electrode. The results are reported in Table 6. The potential and current were increased with increasing surface area, but above 1.0 × 1.0 cm^2 area, both the current as well as potential were decreased.

4.6. Effect of Light Intensity

Light intensity may also affect the electrical output of the cell and therefore, the effect of light intensity was also observed. The results are shown in Table 7. Light intensity was varied from 30 to 70 $mWcm^{-2}$. An increasing trend was observed because an increase in light intensity will increase the number of photon per unit area. The current and potential were found to decrease above 60 $mWcm^{-2}$.

Table 7. *Effect of light intensity.*

Light Intensity ($mWcm^{-2}$)	Potential (mA)	Current (µA)
30	136.1	12.8
40	177.8	15.8
50	235.3	22.5
60	395.0	33.9
70	346.2	25.0

[Rhodamine B] = 1.0 x 10^{-3} M; Electrolyte [I_2] = 0.47 M, [KI] = 0.51 M; Exposed surface area = 1.0 x 1.0 cm^2

4.7. i–V Characteristics of the Cell

The open circuit voltage (V_{oc}), keeping the circuit open and short circuit current (i_{sc}), keeping the circuit closed, were measured by a digital multimeter. The values of photocurrent and photopotential were observed with the help of a carbon pot (log 470 K) connected in the circuit by applying an external load. The results of variation of potential and current are represented in Table 8. and graphically in Fig. 8

Table 8. *i–V characteristics.*

Potential (mV)	Current (µA)	Fill factor
395.0	0.0	
300.0	0.5	
253.0	1.7	
199.1	2.5	
145.7	4.7	
133.2	8.6	
120.8	10.3	
112.8	12.1	
86.1	13.5	
77.7	14.7	
76.1	15.4	
74.9	16.1	
73.1	17.5	
68.9	19.7	
66.2	20.9	0.10
62.0	21.7	
58.6	23.4	
49.1	27.1	
34.7	30.8	
18.2	32.4	
0.0	33.9	

[Rhodamine B] = 1.0 x 10^{-3} M; Electrolyte [I_2] = 0.47 M, [KI] = 0.51 M; Exposed surface area = 1.0 x 1.0 cm^2; Light intensity = 60 $mWcm^{-2}$

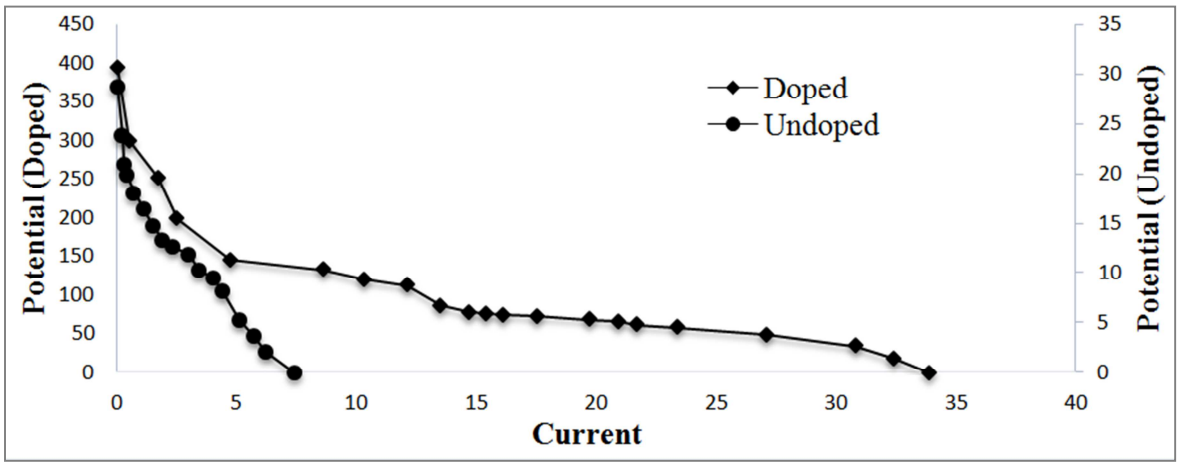

Fig. 10. *Photocurrent-voltage curve of the cell.*

Value of V_{oc}, i_{sc}, V_{pp} (voltage at power point) and i_{pp} (current at power point) were determined with the help of this plot. The maximum voltage at open circuit (V_{oc}) was 395.0 mV and the maximum current at short circuit (i_{sc}) was 0.0339 mA. The (V_{pp}) = 66.2 mV and (i_{pp}) = 0.0209 mA were obtained at power point. Fill factor was calculated by using equation (2) and it was found to be 0.10.

$$\text{Fill Factor} = \frac{V_{pp} \times i_{pp}}{V_{oc} \times i_{sc}} \quad (2)$$

5. Cell Efficiency

The power conversion efficiency (η) of cell is the ratio of electric output at the power point and power of incident radiation (P_{in}). The power conversion efficiency (η) was determined by following equation:

$$\eta = \frac{FF \times V_{oc} \times i_{sc}}{P_{in}} \quad (3)$$

This cell exhibited 0.0023% overall power conversion efficiency. The comparative study of electrical parameters, fill factor and conversion efficiency of co-doped and undoped DSSC are given in Table 9.

Table 9. *Comparative results of pure and Cu/N co-doped TiO_2 in DSSC.*

Sample	i_{pp} (mA)	V_{pp} (mV)	i_{sc} (mA)	V_{oc} (mV)	FF	η x 10^2 (%)
Pure TiO_2	0.0040	9.5	0.0074	28.7	0.17	0.0060
Cu/N–TiO_2	0.0209	66.2	0.0339	395.0	0.10	0.23

6. Conclusion

It is reported that doping of a semiconductor enhances its activity as it lowers its band gap. In the present investigation, two different DSSCs were fabricated using pure TiO_2 and Cu/N─TiO_2. These electrodes were prepared in the laboratory by sol-gel process. The FTIR analysis of these semiconductors confirmed O–H, Ti–O–Ti, Cu–O, Cu–Ti, Ti–N stretching and Cu–N–O bending. XRD and SEM analysis showed that the particle size of the semiconductor was increased on doping TiO_2 by copper and nitrogen. DRS data also confirmed lowering of band gap of TiO_2 when doped with copper and nitrogen. The observations confirmed that the photocatalytic performance of DSSC fabricated with Cu/N─TiO_2 was found better than pure TiO_2. It is also worth mentioning that the performance of Cu/N─TiO_2 cell was enhanced 38 times as compared to pure TiO_2.

Acknowledgement

The authors are thankful to PAHER University, Udaipur for providing necessary laboratory facilities. We are also thankful to Director, SAIF, Punjab University, Chandigarh; University of Kota, Kota; M. S. University of Baroda, Vadodara for providing XRD, TEM, FTIR, DRS and SEM analysis.

References

[1] O'Regan, B., Grätzel, M. A low-cost, high-efficiency solar cell based on dye-sensitized colloidal TiO2 films, Nature, Vol. 353, pp. 737-740, 1991.

[2] Chiba, Y., Islam, A., Watanabe, Y., Komiya, R., Koide, N., Han, L., Dye-sensitized solar cells with conversion efficiency of 11.1%. Japn. J. Appl. Phys. Part 2: Letters, Vol. 45, pp. L638-L640, 2006.

[3] Elangovan, R., Venkatachalam, P. Co-sensitization Promoted Light Harvesting for Dye-Sensitized Solar Cells, J. Inorg. Organomet. Polymer Mater., Vol. 25, pp. 823-831, 2015.

[4] Pang, A. Sun, X. Ruan, H. Li, Y. Dai, S. Wei, M. Highly efficient dye-sensitized solar cells composed of TiO2@SnO2 core-shell microspheres, Nano Energy, Vol. 5, pp. 82-90, 2014.

[5] Eom, T.S., Kim, K.H., Bark, C.W., Choi, H.W., Influence of Fe_2O_3 doping on TiO2 electrode for enhancement photovoltaic efficiency of dye-sensitized solar cells, Mol. Cryst. Liq. Cryst., Vol. 600, pp. 39-46, 2014.

[6] J. Y. Park, K.H. Lee , B. S. Kim, C. S. Kim , S. E. Lee, K. Okuyama, H. D. Jang, and T. O. Kim, Enhancement of dye-sensitized solar cells using Zr/N-doped TiO2 composites as photoelectrodes, RSC Adv., vol. 4, pp. 9946-9952, 2014.

[7] F. Gu, W. Huang , S. Wang, X. Cheng ,Y.Hu, and P. S. Lee, Open-circuit voltage improvement in tantalum-doped TiO2 nanocrystals, Phys. Chem. Chem. Phys., vol. 16, no. 47, pp. 25679-2568, 2014.

[8] Yanan Xie, Niu Huang, Sujian You, Yumin Liu, Bobby Sebo, Liangliang Liang, Xiaoli Fang, Wei Liu, Shishang Guo, Xing-Zhong Zhao, Improved performance of dye-sensitized solar cells by trace amount Cr-doped TiO2 photoelectrodes, J. Power Sources, vol. 224, pp. 168-173, 2013.

[9] Chuen-Shii Chou, Yan-Hao Huang, Ping Wuc, Yi-Ting Kuo, Chemical-photo-electricity diagrams by Ohm's law – A case study of Ni-doped TiO2 solutions in dye-sensitized solar cells, Appl. Energy, vol. 118, pp. 12–21, 2014.

[10] Niu, M. Cui, R. Wu, H. Cheng, D. Cao, D. Enhancement mechanism of the conversion efficiency of dye-sensitized solar cells based on nitrogen, fluorine, and iodine doped TiO2 photoanodes, J. Phys. Chem. C, Vol. 119, pp. 13425-13432, 2015.

[11] C-H. Han, H-S. Lee,K-W. Lee, S-D. Han, and I. Singh, Synthesis of Amorphous Er^{3+}-Yb^{3+} Co-doped TiO_2 and Its Application as a Scattering Layer for Dye-sensitized Solar Cells, Bull. Korean Chem. Soc., Vol. 30, pp. 219-223, 2009.

[12] Duan, Y., Zheng, J., Xu, M., Song, X., Fu, N., Fang, Y., Zhou, X., Lin, Y., Pan, F., Metal and F dual-doping to synchronously improve electron transport rate and lifetime for TiO_2 photoanode to enhance dye-sensitized solar cells performances, J. Mater. Chem. A, vol. 3, pp. 5692-5700, 2015.

[13] R. Ocwelwang and L. Tichagwa, Synthesis and Characterization of Ag and Nitrogen Doped TiO_2 Nanoparticles Supported on A Chitosan-PVAE Nanofibre Support, Int. J. Adv. Res. Chem. Sci., vol. 1, pp. 28-37, 2014.

[14] R. Sharmila Devi, Dr. R. Venckatesh, and Dr. Rajeshwari Sivaraj, Synthesis of Titanium Dioxide Nanoparticles by Sol-Gel Technique, Int. J. Innov. Res. Sci. Eng. Technol., vol. 3, pp. 15206-15211, (2014).

[15] B. V. Rao, A. D. P. Rao and V. Raghavendra Reddy, Influence of Mo^{6+} On Ftir And Mössbauer Spectroscopic Properties of Copper Ferrite, Int. J. Innov. Res. Sci. Eng. Technol, vol. 2, pp. 7768-7779, 2013.

[16] H. Tachikawa, T. Iyama and T. Hamabayashi, Metal–ligand interactions of the Cu–NO complex at the ground and low-lying excited states: an *ab initio*MO study, Electron. J. Theor. CH., vol. 2, pp. 263–267, 1997.

[17] A. Rahmati, Nitrification of Reactively Magnetron Sputter Deposited Ti-Cu Nano-Composite Thin Films, Soft Nanoscience Letters, vol. 3, pp. 14-21, 2013.

[18] H. Diker, C. Varlikli, K. Mizrak, and A. Dana, Characterizations and photocatalytic activity comparisons of N-doped nc-TiO_2 depending on synthetic conditions and structural differences of amine sources, Energy, vol. 36, pp. 1243-1254, 2011.

[19] K. Lv, H. Zuo, J. Sun, K. Deng, S. Liu, X. Li, and D. Wang, (Bi, C and N) codoped TiO_2 nanoparticles, J. Hazard. Mater., vol. 161, pp. 396–401, 2009.